PHYSICAL REVIEW A **87**, 031402(R) (2013)

Approach to form long-range ion-pair molecules in an ultracold Rb gas

Adam Kirrander,[1,2,*] Seth Rittenhouse,[2,3] Marco Ascoli,[4] Edward E. Eyler,[4] Phillip L. Gould,[4] and H. R. Sadeghpour[2]

[1]*School of Chemistry, University of Edinburgh, West Mains Road, Edinburgh EH9 3JJ, United Kingdom*

[2]*ITAMP, Harvard-Smithsonian Center for Astrophysics, Cambridge, Massachusetts 02138, USA*

[3]*Department of Physics and Astronomy, Western Washington University, Bellingham, Washington 98225, USA*

[4]*Physics Department, University of Connecticut, 2152 Hillside Rd., Storrs Connecticut 06269-3046, USA*

(Received 3 February 2013; published 22 March 2013)

We propose a realizable and efficient approach for exciting long-range ion-pair molecules, known as heavy Rydberg states, in an ultracold ^{85}Rb gas via Feshbach resonances. Heavy Rydberg states, the molecular analogs of electronic Rydberg states, with the electron replaced by an atomic anion, offer opportunities for novel physics, including the formation of ultracold anions and strongly coupled plasmas. We map the positions, lifetimes, and Franck-Condon factors of heavy Rydberg resonances across a wide range of excitation energies, and we calculate the rates of formation for the most promising transitions through long-lived intermediate interferometric resonances.

DOI: 10.1103/PhysRevA.87.031402 PACS number(s): 32.80.Ee, 33.20.Wr, 33.80.Gj

Exotic molecular ion-pair states (heavy Rydberg states) are the analog of electronic Rydberg states with the electron replaced by an atomic anion. They have unusual properties, including extremely long-range vibrations, large dipole moments, and a near-infinite manifold of vibrational states. Heavy Rydberg states (HRS) in an ultracold gas may provide interesting opportunities for Doppler-free high-precision spectroscopy, formation of the first ultracold atomic and molecular anions, accurate determination of the atomic electron affinity, and control of wave packets with lifetimes exceeding 100 ns. Most intriguing is, perhaps, the formation of ultracold strongly coupled two-component plasmas with the light and fast electrons replaced by ultracold atomic anions.

Heavy Rydberg states have been realized in crossed-beam experiments [1–3] and above the ion-pair dissociation threshold [4–6]. On the other hand, all recent spectroscopic studies [7–10] rely on the excitation of short-range complex resonances, which act as gateway states and populate the long-range HRS via nonadiabatic couplings. Such indirect excitation pathways are required because of the extremely small Franck-Condon overlap between normal vibrational states and the very-long-range HRS. Although indirect excitation pathways have been identified in both H_2 and Cl_2 at energies convenient for spectroscopy, there is at present no reliable way to predict where and if such complex resonances appear. Furthermore, neither H nor Cl are suited to modern cooling techniques.

In contrast, cooling and trapping of Rb is now routine. However, no complex resonances in Rb_2 leading to HRS have yet been identified, despite the observation of Rb_2 ion-pair satellite bands in absorption measurements in hot dense Rb vapor [11]. A possible excitation route for HRS would be via intermediate long-range vibrational states. Unfortunately, the exceedingly small dipole transition moment for laser excitation into the HRS manifold, due to the weak covalent-to-ionic transition at large internuclear distances, is a problem.

In this work, we suggest a realizable and efficient approach to excite HRS directly, and demonstrate its formation and efficiency by theoretical calculations for Rb_2. The scheme relies on direct excitation from Feshbach resonances or weakly bound vibrational states in an ultracold ^{85}Rb gas to HRS resonances just below the avoided crossings between covalent potential-energy curves and the long-range Coulombic ion-pair potential. These below-threshold states have long lifetimes, and the nonadiabatic mixing at the avoided crossings provides favorable dipole transition moments from the Feshbach resonance to the HRS. Although our approach results in comparatively low-lying HRS, further excitation to states with very high principal quantum number is readily possible via adiabatic rapid passage using microwave fields, either by chirped pulses [12] or multiphoton transitions [13].

We calculate the positions and lifetimes of HRS resonances in Rb_2 by solving the nonadiabatic close-coupled equations for nuclear motion on the *ab initio* potential-energy curves for states $1-7\,^1\Sigma_g^+$ from Park *et al.* [14], shown in Fig. 1. The ion-pair potential included in Fig. 1 is given in a.u. by

$$V_{\rm ion}(R) = D_{\rm Rb^+Rb^-} - \frac{1}{R} - \frac{\alpha_{\rm Rb^+} + \alpha_{\rm Rb^-}}{2R^4}, \qquad (1)$$

where the polarizabilities are $\alpha_{\rm Rb^+} = 9.11$ a.u. [15] and $\alpha_{\rm Rb^-} = 526.0$ a.u. [16], with the experimental ion-pair dissociation energy $D_{\rm Rb^+Rb^-} = 29\,771.59\ {\rm cm}^{-1}$ [17,18]. Only the $^1\Sigma_g^+$ and $^1\Sigma_u^+$ symmetries support ion-pair states, corresponding to 0_g^+ and 0_u^+ states when accounting for spin-orbit coupling. In these calculations, we account for the coupling of the ion-pair potential and the covalent Rydberg potential curves near $R_c = 38$ a.u. and 52 a.u. by constructing the respective matrix elements. Our calculations focus on the five highest-energy *ab initio* potential-energy curves (PECs) shown in Fig. 1 and the ion-pair potential given by Eq. (1). The two lowest $^1\Sigma_g^+$ PECs are separated from the rest by a large energy and therefore have insignificant influence on the dynamics. Chibisov *et al.* report on asymptotic exchange interactions and couplings [19], but since radial nonadiabatic coupling matrix elements have been unavailable until very recently [20], we fit the nonadiabatic couplings at each avoided crossing using

*adam.kirrander@ed.ac.uk

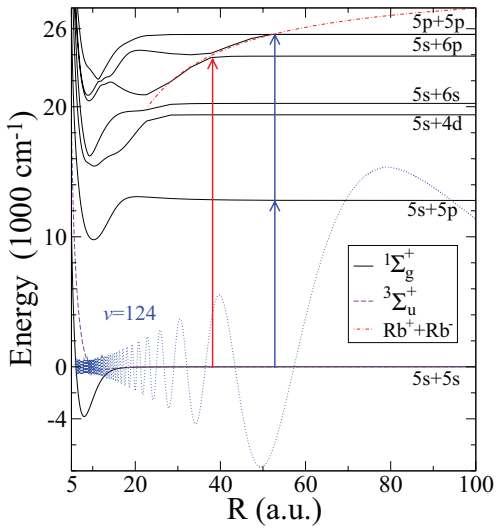

FIG. 1. (Color online) *Ab initio* potential-energy curves (PECs) for Rb_2 from Park *et al.* [14]. The first seven adiabatic PECs and the ion-pair potential [see Eq. (1)] are shown for the symmetry $^1\Sigma_g^+$, and the lowest PEC for $^3\Sigma_u^+$. The last bound vibrational wave function $v = 124$ in the ground state $X^1\Sigma_g^+$ potential, which closely resembles the Feshbach resonance on the lowest $^1\Sigma_g^+$ and $^3\Sigma_u^+$ PECs, is shown, as well as the one-photon excitation to states below the $5s + 6p$ and the two-photon transition to states below the $5p + 5p$ threshold near the avoided crossings with the ion-pair potential.

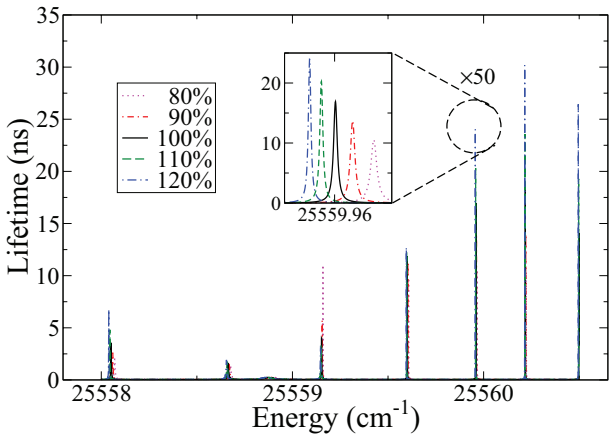

FIG. 2. (Color online) Stability of calculated spectrum with respect to variation of strength of nonadiabatic couplings by ±10% and ±20% (a region in the spectrum below the $5p + 5p$ dissociation limit is shown). The positions of the resonances change little as a function of the couplings, but the lifetimes are more sensitive due to the interferometric nature of the resonances, as can be seen in the blowup of the resonance at 25 559.96 cm^{-1}.

a two-state approximation [21]. Our couplings are in general accord with those reported in Ref. [20]. The resulting set of diabatic states and couplings reproduce the adiabatic *ab initio* potentials accurately. In effect, this approach closely resembles the Landau-Zener approximation [22]. In total, seven sets of two-state avoided crossings are included. The results of these calculations remain reasonably stable with respect to variations in the strength of the couplings by up to ±30%, in particular in terms of the positions of resonances, as can be seen in Fig. 2. Note, however, that the calculated lifetimes are more sensitive to changes in the nonadiabatic couplings, indicative of the interferometric nature of the resonances (see Ref. [23] and below).

We solve the close-coupled equations for nuclear motion in the standard diabatic representation,

$$\boldsymbol{\Psi}''(R) = \boldsymbol{W}(R)\boldsymbol{\Psi}(R), \tag{2}$$

with $\boldsymbol{\Psi}$ being an $N \times N$ matrix, each column a linearly independent solution, and $\boldsymbol{\Psi}''$ indicating the second derivative with respect to R. The matrix $\boldsymbol{W}$ consists of

$$\boldsymbol{W}(R) = \frac{2M}{\hbar^2}\boldsymbol{V}(R) - \boldsymbol{k}^2, \tag{3}$$

where the $N \times N$ matrix $\boldsymbol{V}$ contains the diagonal potentials and the off-diagonal coupling elements. The diagonal matrix $\boldsymbol{k}$ contains the asymptotic channel wave vectors $\boldsymbol{k}^2 = (2M/\hbar^2)\boldsymbol{\epsilon}$ where M is the reduced mass of $^{85}Rb_2$ and $\boldsymbol{\epsilon}$ is a diagonal matrix such that $\epsilon_i = E - E_i$, where E is the total energy and E_i is the threshold energy in each channel i.

Equation (2) is solved using the log-derivative method [24], which propagates the log-derivative matrix $\boldsymbol{Y}(R) = \boldsymbol{\Psi}'(R)\boldsymbol{\Psi}^{-1}(R)$ instead of propagating the wave function $\boldsymbol{\Psi}$ directly. The matrix is propagated out to the matching radius R_f, where it is used to calculate the wave function in the form $\boldsymbol{\Psi} = \boldsymbol{F} - \boldsymbol{G}\boldsymbol{K}$, where $\boldsymbol{F}$ and $\boldsymbol{G}$ are diagonal $N \times N$ matrices containing energy-normalized Milne functions [25]. These coincide with analytic Coulomb and Riccati-Bessel functions when the polarization term in Eq. (1) vanishes. The density of states is calculated from the energy derivative of the cumulative eigenphase of the scattering matrix. The lifetimes τ are obtained from the width at half maximum, Γ, for each resonance.

Figure 3 shows the lifetimes of the resonances in the energy range 23 815 to 25 601 cm^{-1}, beginning below the $5s + 6p$ limit and continuing up above the $5p + 5p$ limit. They are shown in terms of their lifetimes, since this is a crucial aspect when choosing a suitable target state for excitation. Each calculated resonance can be assigned a principal quantum number n_{IP} and a quantum defect μ by reference to the Rydberg formula (see, e.g., Ref. [26]). The overall progression of states in the calculated range corresponds to that typical of low-lying heavy Rydberg states, with a strong energy dependence of the quantum defects and many interloper states [26,27]. The slow transition to "pure" HRS behavior in terms of quantum defects and density of states, compared with electronic Rydberg states, can be attributed to the large reduced mass and the extensive range of internuclear distances where the potentials deviate significantly from the pure Coulomb potential. The resonances display the same interferometric modulations of the lifetimes that were previously observed in LiF [23]. The large reduced mass and the large internuclear separation make the heavy Rydberg states robust with regard to changes in the total angular momentum J, with only very small shifts in resonance positions due to changes in the rotational angular momentum. We therefore anticipate little thermal broadening and rotational dependence of the formation rates.

Our excitation scheme relies on a vertical transition from a Feshbach resonance in the lowest $^1\Sigma_g^+$ and $^3\Sigma_u^+$ electronic states directly into heavy Rydberg resonances in the excited

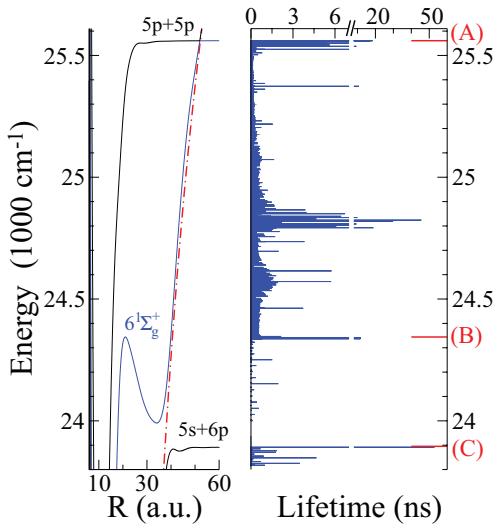

FIG. 3. (Color online) Calculated lifetimes for resonances in $Rb_2(^1\Sigma_g^+)$ plotted as a function of energy and mapped against the PECs in the range 23 815 to 25 601 cm^{-1}, which begins below the $5s + 6p$ dissociation limit and ends above the $5p + 5p$ limit. The states in the gap between the $5s + 6p$ dissociation limit and the minimum of the outer well in $6^1\Sigma_g^+$ (labelled in the graph) have short-range character. These are followed by a region below the inner barrier of $6^1\Sigma_g^+$ with a low density of states. The comparatively long-lived resonances just below the $5s + 6p$ and the $5p + 5p$ dissociation limits have reasonable dipole transition moments from the Rb_2 Feshbach resonance. Labels A and C indicate the positions in the spectrum of the avoided crossings between the ion-pair potential and the $5p + 5p$ and $5s + 6p$ states, respectively, while B indicates the height of the inner barrier on the lower of the two PECs that go to the $5p + 5p$ limit. The ion-pair potential from Eq. (1) is included for reference (dot-dashed line).

$^1\Sigma_g^+$ manifold, which we take as representative of the 0_g^+ and 0_u^+ symmetries that support the heavy Rydberg states. The wave function for the Feshbach resonance is well approximated by the wave function for the last bound $v = 124$ vibrational state on the *ab initio* ground-state $X^1\Sigma_g^+$ potential, accounting for all of the higher-order dispersion interaction terms (C_{2n}/R^{2n} with $n = 3,4,5,\ldots$) [28]. The corresponding vibrational wave function in the $^3\Sigma_u^+$ potential is similar in the region of large R. Heavy Rydberg states just below the $5s + 6p$ and $5p + 5p$ dissociation limits are comparatively long lived and have good Franck-Condon overlaps with the Feshbach resonance due to the large lobe at their classical outer turning point, R_{tp}, on the ion-pair potential. The wave functions for the resonances are not immediately obtained from the log-derivative calculations, but must be calculated separately for each resonance by inward propagation from the asymptotic scattering wave function.

In general, the dipole moments from the covalent initial state to the ionic HRS are weak, but the HRS with turning points R_{tp} close to the nonadiabatic crossing R_c with the ion-pair potential benefit from strong mixing between the covalent and ionic PECs at the location of maximum Franck-Condon overlap. Close to the avoided crossings, the heavy Rydberg wave function $\Psi_{hrs}(R)$ is a superposition of covalent and ionic components,

$$\Psi_{hrs}(R) = \sin\xi(R)\Psi_{cov}(R) + \cos\xi(R)\Psi_{ion}(R), \quad (4)$$

where the mixing angle $\xi(R)$ due to the avoided crossing between i and j is given by the first-derivative radial coupling term $A_{ij}(R)$,

$$\xi(R) = \int_R^\infty A_{ij}(R')\,dR'. \quad (5)$$

To a good approximation, the transition moment from the Feshbach resonance to the HRS can be written as

$$D_{hrs,i} = f_{hrs,i}\sin\xi(R_{tp})D_{cov,i}, \quad (6)$$

assuming that the covalent-covalent dipole transition moment is much larger than the covalent-ionic moment, $D_{cov,i} \gg D_{ion,i}$, and that the Franck-Condon overlap $f_{hrs,i}$ is dominated by the wave function close to the classical turning point where its amplitude is the largest.

For resonances just below the $5s + 6p$ dissociation limit, near the avoided crossing around $R_c = 38$ a.u., the relevant covalent transition moment is proportional to the atomic $d_{5s\to6p}$ transition and a single-photon transition from the initial Feshbach resonance to the final state is possible. The single-photon Rabi frequency Ω_1 for this process is

$$\Omega_1 = |E d_{5s\to6p} f_{hrs,i}\sin\xi|, \quad (7)$$

where $E = (\frac{8\pi}{c}I)^{1/2}$ is the laser electric field strength with I being the laser intensity, $d_{5s\to6p} = (\frac{3}{4}\frac{\omega^3}{c^3}A_{5s\to6p})^{1/2} = 0.244$ a.u. is the dipole matrix element using the Einstein A coefficient $A_{5s\to6p} \approx 1.64 \times 10^5\ s^{-1}$, and $f_{hrs,i}$ and ξ are the Franck-Condon overlap and the covalent-ionic mixing angle listed in Table I, respectively. For modest intensities, $I = 10^3\ W/cm^2$, the single-photon Rabi frequency is on the order $\Omega_1 \sim 2\pi \times 10^2$ kHz. This is quite promising, especially given that the laser intensity can be increased.

For the states below the $5p + 5p$ limit, with $R_c = 51.97$ a.u., a two-photon transition is required. The two-photon

TABLE I. Heavy Rydberg resonances suitable for excitation, located below the crossings between V_{ion} and $5s + 6p$ (at $R_c = 38$ a.u., $\Delta E \sim 300\ cm^{-1}$) and $5p + 5p$ (at $R_c = 51.97$ a.u., $\Delta E \sim 3\ cm^{-1}$). The resonance position in cm^{-1}, lifetime τ in ns, classical turning point R_{tp}, the Franck-Condon overlap $f_{hrs,i}$, and the mixing angle ξ between the covalent and ionic potentials at R_{tp} are given. We include the excitation rates calculated using Eq. (9) with the single-photon Rabi frequency Eq. (7) for states with $R_{tp} \approx 38$, or the two-photon Rabi frequency Eq. (8) for states with $R_{tp} \approx 52$.

Energy (cm^{-1})	τ (ns)	R_{tp} (a.u.)	$\lvert f_{hrs,i}\rvert$	ξ (rad)	Rate ($10^3 \times s^{-1}$)
23 825.64*	3.49	38.43	0.016	−0.087	121
23 847.97	4.68	38.89	0.020	−0.042	58
25 555.71	5.04	51.91	0.039	−1.140	139
25 556.99	4.22	51.93	0.058	−1.038	239
25 559.60*	11.95	52.01	0.064	−0.528	313
25 559.96	17.09	52.09	0.060	−0.281	118
25 560.22	18.45	53.45	0.058	−0.025	1

Rabi frequency Ω_2 is

$$\Omega_2 = \frac{|E d_{5s\to 5p}|^2}{\Delta} |f_{\mathrm{hrs,i}} \sin\xi|, \tag{8}$$

where Δ is the detuning from the intermediate state. If we assume that the both photons come from the same laser and that the detuning is half the final-state energy with respect to the $5p + 5p$ threshold, giving a detuning of approximately $\Delta \approx 40\ \mathrm{cm}^{-1}$, we have $d_{5s\to 5p} = (\frac{3}{4}\frac{\omega^3}{c^3} A_{5s\to 5p})^{1/2} = 2.99$ a.u., using $A_{5s\to 5p} = 3.81 \times 10^7\ \mathrm{s}^{-1}$. The mixing angles ξ and the Franck-Condon overlap $f_{\mathrm{hrs,i}}$ are taken from Table I. Again, using modest intensities, $10^3\ \mathrm{W/cm}^2$, excellent Rabi frequencies $\Omega_2 \sim 2\pi \times 10^2$ kHz are obtained. Since the intermediate state is far detuned, the laser intensity can be further increased without significant ionization, up to 10^7–$10^9\ \mathrm{W/cm}^2$.

Using Fermi's golden rule, the rate $\mathcal{R}$ is obtained as

$$\mathcal{R} = 2\pi\Omega^2\tau, \tag{9}$$

where τ is the lifetime and the resonances are treated as having Lorentzian shapes. If we illuminate a sample of trapped $^{85}Rb_2$ molecules with 10 ns pulses of 100 mW peak power focused to a diameter of 100 μm, the HRS excitation probability per shot will be on the order of 10^{-5}–10^{-3} per molecule, using the rates from Table I. We note here an important advantage of starting with bound molecules instead of trying to produce HRS by photoassociation from the continuum: the existence of a Franck-Condon window in R which can be varied by choice of the initial molecular state.

In conclusion, we propose a scheme for exciting heavy Rydberg states in an ultracold ^{85}Rb gas. It relies on direct excitation from Feshbach resonances or weakly bound molecules to heavy Rydberg states (HRS) just below the avoided crossings between covalent potential-energy curves and the long-range ion-pair potential. Purely ionic HRS can form by, for instance, stepwise excitation using a chirped laser pulse and can be detected by field ionization. These states have long lifetimes, and the nonadiabatic mixing at the avoided crossings provides favorable dipole transition moments. In the future, we anticipate being able to improve the predictions by including *ab initio* couplings and to account for spin-orbit interactions.

This work was supported by the National Science Foundation through a grant for the Institute for Theoretical Atomic, Molecular, and Optical Physics at Harvard University and Smithsonian Astrophysical Observatory and by a National Science Foundation grant to the University of Connecticut. We are grateful to Z. Pavlović for the calculations of the wave functions for the Feshbach resonances. The authors acknowledge helpful discussions with S. Yelin and E. Kuznetsova, as well as G. Pichler (H.R.S.), K. Lawley and T. Ridley (A.K.), and B. L. Johnson (S.R.).

[1] M. Cannon, C. H. Wang, Y. Liu, F. B. Dunning, and J. D. Steill, J. Chem. Phys. **130**, 244311 (2009).
[2] M. Cannon, C. Wang, and F. Dunning, Chem. Phys. Lett. **479**, 30 (2009).
[3] M. Cannon, C. H. Wang, F. B. Dunning, and C. O. Reinhold, J. Chem. Phys. **133**, 064301 (2010).
[4] W. A. Chupka, P. M. Dehmer, and W. T. Jivery, J. Chem. Phys. **63**, 3929 (1975).
[5] X. Liu, R. L. Gross, and A. G. Suits, Science **294**, 2527 (2001).
[6] A. Suits and J. W. Hepburn, Ann. Rev. Phys. Chem. **57**, 431 (2006).
[7] M. O. Vieitez, T. I. Ivanov, E. Reinhold, C. A. de Lange, and W. Ubachs, Phys. Rev. Lett. **101**, 163001 (2008).
[8] M. O. Vieitez, T. I. Ivanov, E. Reinhold, C. A. de Lange, and W. Ubachs, J. Phys. Chem. A **113**, 13237 (2009).
[9] R. C. Ekey, Jr. and E. F. McCormack, Phys. Rev. A **84**, 020501 (2011).
[10] S. Mollet and F. Merkt, Phys. Rev. A **82**, 032510 (2010).
[11] T. Ban, R. Beuc, H. Skenderović, and G. Pichler, Eur. Phys. Lett. **66**, 485 (2004).
[12] J. Lambert, M. W. Noel, and T. F. Gallagher, Phys. Rev. A **66**, 053413 (2002).
[13] H. Maeda, J. H. Gurian, D. V. L. Norum, and T. F. Gallagher, Phys. Rev. Lett. **96**, 073002 (2006).
[14] S. J. Park, S. W. Suh, Y. S. Lee, and G.-H. Jeung, J. Mol. Spectrosc. **207**, 129 (2001).
[15] J. Mitroy, M. S. Safronova, and C. W. Clarke, J. Phys. B **43**, 202001 (2010).
[16] I. I. Fabrikant, J. Phys. B **26**, 2533 (1993).
[17] C. E. Moore, Natl. Stand. Ref. Data Ser. (US Natl. Bur. Stand.) **34**, 1 (1970).
[18] P. Frey, F. Breyer, and H. Hotop, J. Phys. B **11**, L589 (1978).
[19] M. I. Chibisov and R. K. Janev, Phys. Rep. **166**, 1 (1988).
[20] M. Tomza, W. Skomorowski, M. Musiał, R. González-Férez, C. P. Koch, and R. Moszynski, arXiv:1301.4966.
[21] E. F. van Dishoeck, M. C. van Hemert, A. C. Allison, and A. Dalgarno, J. Chem. Phys. **81**, 5709 (1984).
[22] C. W. Clarke, Phys. Lett. A **70**, 295 (1979).
[23] S. T. Cornett, H. R. Sadeghpour, and M. J. Cavagnero, Phys. Rev. Lett. **82**, 2488 (1999).
[24] D. E. Manolopoulos, J. Chem. Phys. **85**, 6425 (1986).
[25] C. Jungen and F. Texier, J. Phys. B **33**, 2495 (2000).
[26] A. Kirrander, J. Chem. Phys. **133**, 121103 (2010).
[27] A. Kirrander and C. Jungen, Phys. Rev. A **84**, 052512 (2011).
[28] M. Marinescu and A. Dalgarno, Phys. Rev. A **52**, 311 (1995).